DYNAMIC ANALYSIS OF
DOUBLE WISHBONE SUSPENSION

**A Thesis Submitted to
the Graduate School of Engineering and Sciences of
İzmir Institute of Technology
in Partial Fulfillment of the Requirements for the Degree of**

MASTER OF SCIENCE

in Mechanical Engineering

**by
Duygu GÜLER**

**July 2006
İZMİR**

We approve the thesis of **Duygu GÜLER**

....

07 July 2006

Assoc. Prof. Dr. Bülent YARDIMOĞLU

Supervisor

Department of Mechanical Engineering

İzmir Institute of Technology

....

07 July 2006

Assist. Prof. Dr. Engin AKTAŞ

Department of Civil Engineering

İzmir Institute of Technology

....

07 July 2006

Assist. Prof. Dr. Cemalettin DÖNMEZ

Department of Civil Engineering

İzmir Institute of Technology

....

07 July 2006

Assoc. Prof. Dr. M. Barış ÖZERDEM

Head of Department

İzmir Institute of Technology

....

Assoc. Prof. Dr.Semahat ÖZDEMİR

Head of the Graduate School

ACKNOWLEDGEMENTS

ABSTRACT

DYNAMIC ANALYSIS OF DOUBLE WISHBONE SUSPENSION

In this study, the natural frequencies, body displacements, velocities, and accelerations of a quarter-car with double wishbone suspension are examined by considering the proportionally damped system. Two models of quarter-car suspension system are idealized employing two different assumptions due to the suspension links to describe the dynamic behaviour of vehicles running on base excitation. In the first model, the links of the suspension are assumed to be rigid and the stiffness and mass matrices of the model are obtained by using the analytical method. In the second model, the links of the suspension are assumed to be flexible and the elastic stiffness, mass, and geometric stiffness matrices are obtained by using Finite Element Method. In order to express the linear equation of motion, suspension link forces required for the geometric stiffness matrices are assumed as constant. Also, the oscillations of the suspension links are neglected since the base displacement is chosen in small amplitude.

Two Matlab programs regarding the aforementioned models have been developed. Firstly, the natural frequencies of the models are found. Then, the displacements, velocities, and acceleration of the car body are presented in graphical forms for the specified car speed. The excellent agreement between results of the analytical model and finite element model is observed for both natural frequencies and the time reponses. The effect of loads on suspension link on the dynamic behaviour of suspension system is also studied.

ÖZET

ÇİFT ENİNE YÖN VERİCİ ASKI SİSTEMİNİN DİNAMİK ANALİZİ

Bu çalışmada, çift enine yön vericili çeyrek bir aracın doğal frekansları, gövdenin yerdeğiştirme, hız ve ivmeleri oransal sönümlü bir sistem gözönüne alınarak incelenmiştir. İki çeyrek-araç süspansiyon sistemi modeli zemin uyarısı altındaki bir aracın dinamik davranışını tanımlamak için süspansiyon uzuvları dolayısıyla iki değişik kabul kullanılarak modellenmiştir. Birinci modelde, süspansiyonun uzuvları rijit olarak kabul edilip kütle ve direngenlik matrisleri analitik method ile elde edilmiştir. İkinci modelde, süspansiyon uzuvları esnek olarak kabul edilmiş ve elastik direngenlik, kütle ve geometrik direngenlik matrisleri sonlu elemanlar methodu ile elde edilmiştir. Hareket denklemini lineer olarak ifade etmek için geometrik direngenlik matrisi için gerekli olan süspansiyon uzuv kuvvetleri sabit olarak kabul edilmiştir. Ayrıca süspansiyon uzuvlarının salınımı zemin yerdeğiştirmesinin küçük genlikte seçilmesinden dolayı ihmal edilmiştir.

Bahsedilen modellerle ilgili iki Matlab programı geliştirilmiştir. İlk olarak, modellerin doğal frekansları bulunmuştur. Daha sonra, araç gövdesinin yerdeğiştirme, hız ve ivmeleri belirlenmiş araç hızları için grafiksel formlarda sunulmuştur. Hem doğal frekanslar hem de zaman cevapları için analitik ve sonlu eleman modellerinin sonuçları arasında mükemmel uyum gözlenmiştir. Süspansiyon uzuvlarındaki yüklerin süspansiyonun dinamik davranışına etkisi de çalışılmıştır.

TABLE OF CONTENTS

LIST OF FIGURES

LIST OF TABLES

LIST OF SYMBOLS

a	Vehicle acceleration
a_1, a_2	Proportional damping coefficients
A	Cross sectional area
$[A]$	State matrix
b	Width of vehicle
B	Front axle track width
c_D	Aerodynamic drag coefficient
$[C]$	Global damping matrix
d	Diameter of the helical spring
E	Modulus of elasticity
f_R	Rolling resistance coefficient
f_s	Friction coefficient between the road and tire
$[f]$	Column matrix of forces
g	Gravity
G	Weight of vehicle
G_{dyn}	Maximum dynamic load on the front tyre
G_{FA}	Static load on the front axle
G_{FAdyn}	Dynamic load on the front axle
G_{RA}	Static load on the rear axle
G_{RAdyn}	Dynamic load on the rear axle
G_{FAw}	Static load on the one wheel
G_{LSdyn}	Dynamic load on the left side of vehicle
G_{RSdyn}	Dynamic load on the right side of vehicle
G_s	Shear modulus of the spring material
h	Height of vehicle
H	Height of center of gravity
I	Area moment of inertia of the cross section
k_t	Tire stiffness value
k	Suspension spring stiffness value

$[\widetilde{k}]$	Element elastic stiffness matrix
$[\widetilde{k}_s]$	Spring stiffness matrix
$[K]$	Global elastic stiffness matrix
l	Length of vehicle
ℓ	Length of the plane frame element
L	Wheelbase of vehicle
L_F	Distance from front axle to CG
L_R	Distance from rear axle to CG
L_r	Period of road profile
m	Vehicle mass (loaded)
m_t	Tire mass value
m_c	Car body mass value
$[\widetilde{m}]$	Element mass matrix
$[M]$	Global mass matrix
n	Number of turns of spring coil
$[N(\xi)]$	Matrix of displacement function
P	Axial load
R	Radius of turn
R_s	Radius of spring coil
r_z	Radius of gyration of the cross-section about the z-axis
$[\widetilde{s}]$	Element geometric stiffness matrix
$[S]$	Global geometric stiffness matrix
S_{dyn}	Lateral force on the front axle right tyre
t	Time
T	Kinetic energy
$\{q\}$	Global displacement vector
u	Axial displacement
U	Total Strain energy
U_e	Elastic strain energy
U_g	Geometric strain energy
v	Transverse displacement
V	Vehicle speed

w_e	Frequency of base excitation
w	Natural frequency
Y	Magnitude of the excitation
θ	Slope or rotation of plane frame element
ρ	Mass per unit volume
ρ_a	Air density
α	The angle of the slope with the horizontal
δ	Angle of upper suspension arm
ξ	Damping ratio

CHAPTER 1

INTRODUCTION

Suspension systems have been widely applied to vehicles, from the horse-drawn carriage with flexible leaf springs fixed in the four corners, to the modern automobile with complex control algorithms. The suspension of a road vehicle is usually designed with two objectives; to isolate the vehicle body from road irregularities and to maintain contact of the wheels with the roadway.

Isolation is achieved by the use of springs and dampers and by rubber mountings at the connections of the individual suspension components.

From a system design point of view, there are two main categories of disturbances on a vehicle, namely road and load disturbances. Road disturbances have the characteristics of large magnitude in low frequency (such as hills) and small magnitude in high frequency (such as road roughness). Load disturbances include the variation of loads induced by accelerating, braking and cornering. Therefore, a good suspension design is concerned with disturbance rejection from these disturbances to the outputs. Roughly speaking, a conventional suspension needs to be "soft" to insulate against road disturbances and "hard" to insulate against load disturbances. Therefore, suspension design is an art of compromise between these two goals (Wang 2001).

Today, nearly all passenger cars and light trucks use independent front suspensions, because of the better resistance to vibrations. One of the commonly used independent front suspension system is referred as double wishbone suspension.

In the literature, a number of studies exist dealing with the double wishbone suspension system. A sample of the relevant literature is as follows:

İbrahim Esat described a method for optimization of the motion characteristics of a double wishbone front suspension system by using a genetic algorithm. The analysis considered only the kinematics of the system (Esat 1999).

T.Yamanaka, H.Hoshino, K. Motoyama developed prototype of optimization system for typical double wishbone suspension system based on genetic algorithms. In this system, the suspension system was analyzed and evaluated by mechanical system simulation software ADAMS (Yamanaka, Hoshino and Motoyama 2000).

Hazem Ali Attia presented dynamic modelling of the double wishbone motor-vehicle suspension system using the point-joint coordinates formulation. In his paper, the double wishbone suspension system is replaced by an equivalent constrained system of 10 particles. Then the laws of particle dynamics are used to derive the equations of motion of the system (Attia 2002).

The aim of this study is to find the effects of link flexibilities and axial link loads on the natural frequencies and also to obtain the vibration displacements, velocities, and accelerations of the car body for different suspension models under typical sinusoidal base excitations. The quarter car with the double wishbone suspension system is modelled for two different approaches to the suspension links to be rigid and flexible. Therefore, the dynamic analyses of these models are investigated by the analytic method and the finite element method. Matlab computer programs have been developed for numerical calculations.

This study consists of five chapters. Chapter 2 introduces the suspension systems and examines vehicle dynamics. Solid axle and independent suspension systems are presented. Double wishbone suspension system is introduced in detail. Vehicle dynamics under different cases and kinetic analysis of double wishbone suspension are examined. Chapter 3 deals with the analytical method and the finite element method. The element stiffness, the mass and the geometric matrices are explained for the plane frame element respectively. Modelling of double wishbone suspension is presented in two models. Vibrations of the double wishbone suspension system, natural frequencies and response to base excitation are studied. Chapter 4 applies the finite element and analytical method to the double wishbone suspension models which are the topics of chapter 3. Results of the kinetic analysis of the double wishbone suspension and results of the vibration analysis of the two models are examined. Conclusion is presented in Chapter 5.

CHAPTER 2

DYNAMICS OF SUSPENSION SYSTEMS

2.1. Introduction to Suspension Systems

The primary functions of a vehicle's suspension systems are to isolate the structure and the occupants from shocks and vibrations generated by the road surface.

The suspension systems basically consist of all the elements that provide the connection between the tires and the vehicle body and are designed to meet the following requirements: (1) Ride comfort, (2) Road-holding, and (3) Handling.

The first requirement mentioned above for the suspension system requires an elastic resistance to absorb the road shocks. This primary function is fulfilled by the suspension springs. Various different types of springs have been used in vehicle suspensions such as leaf springs, helical coil springs, torsion bar springs, air springs, rubber springs.

It is obvious that a suspension system must be able to withstand the loads acting on it. These forces may be in the longitudinal direction such as acceleration and braking forces, in the lateral direction such as cornering forces, and in the vertical direction.

This chapter consists of two main sections. In the first section, the types of suspension systems are introduced and the advantages of double wishbone suspension system are presented. In the second section, vehicle dynamics are presented under different cases in order to obtain axial loads on the double wishbone suspension links.

2.2. Types of Suspension Systems

Suspensions generally fall into either of two groups-solid axles and independent suspensions. Each group can be functionally quite different, and so will be itemized accordingly for discussion.

2.2.1. Solid Axle Suspension Systems

In solid axle suspension systems, wheels are mounted at the ends of a rigid beam so that any movement of one wheel is transmitted to the opposite wheel causing them to steer and camber together.

Solid drive axles are used on the rear of many cars and most trucks and on the front of many four-wheel-drive trucks. Solid beam (non-driven) axles are commonly used on the front of heavy trucks where high load-carrying capacity is required.

Solid axles have the advantage that wheel camber is not affected by body roll. Thus there is little wheel camber in cornering, except for that which arises from slightly greater compression of the tires on the outside of the turn. In addition, wheel alignment is readily maintained, minimizing tire wear. The major disadvantage of solid steerable axles is their susceptibility to tramp-shimmy steering vibrations. The most common solid axles are Hotchkiss, Four link and De Dion.

2.2.2. Independent Suspension Systems

In contrast to solid axles, independent suspensions allow each wheel to move vertically without affecting the opposite wheel. Nearly all passenger cars and light trucks use independent front suspensions, because of the advantages in providing room for the engine and the better resistance to steering vibrations. The independent suspension also has the advantage that it provides inherently higher roll stiffness relative to the vertical spring rate. Further advantages include easy control of the roll centre by choice of the geometry of the control arms, larger suspension deflections, and greater roll stiffness for a given suspension vertical rate.

Over the years, many types of independent front suspension have been tried such as MacPherson, Trailing arm, Swing axle, Multi link and Double wishbone suspension. Many of them have been discarded for a variety of reasons, with only two basic concepts, the double wishbone and the MacPherson strut, finding widespread success in many varied forms.

Double wishbone Suspension (SLA, A-arms)

The most common design for the front suspension of American car following World War II used two lateral control arms to hold the wheel. The upper and lower control arms are usually of unequal length from which the acronym SLA (short-long arm) gets its name.

These are often called "A-arms" in the United States and "wishbones" in Britain. This layout sometimes appears with the upper. A-arm replaced by a simple link, or the lower arm replaced by a lateral link, the suspensions are functionally similar. The SLA is well adapted to front-engine, rear-wheel-drive cars because of the package space it provides for the engine oriented in the longitudinal direction.

Design of the geometry for a SLA requires careful refinement to give good performance. The camber geometry of an unequal-arm system can improve camber at the outside wheel by counteracting camber due to body roll, but usually carries with it less-favourable camber at the inside wheel (equal-length parallel arms eliminate the unfavourable condition on the inside wheel but at the loss of camber compensation on the outside wheel). At the same time, the geometry must be selected to minimize tread change to avoid excessive tire wear (Gillespie 1992).

The compact design of a coil spring makes it ideal for use in front suspension systems. Two types of coil spring mountings are used. In the first type the spring is positioned between the frame and the lower control arm as shown in Figure 2.1. This mounting is most often used on cars with a conventional frame or a partial front frame. The second type of mounting is shown in Figure 2.2. In this mounting, the coil spring is positioned between the upper control arm and a spring tower formed in the inner section of the fender (Remling 1983).

The wishbones may or may not be equal or parallel. The wishbones are parallel and equal in length as shown in Figure 2.3.(a). The parallel and unequal length wishbone suspension system is shown in Figure 2.3.(b). A further refinement is the non-parallel, unequal length wishbone suspension system illustrated in Figure 2.3.(c) (Ünlüsoy 2000).
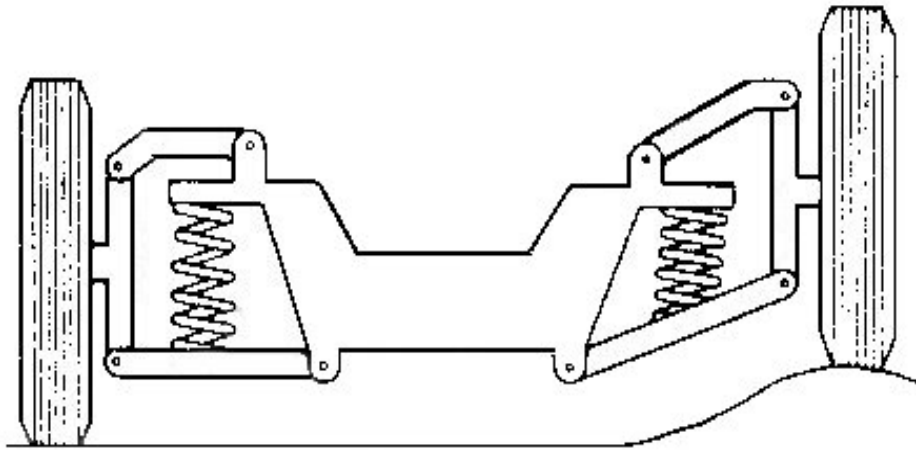
Figure 2.1. A first type of independent front suspension system
(Source: Remling 1983)
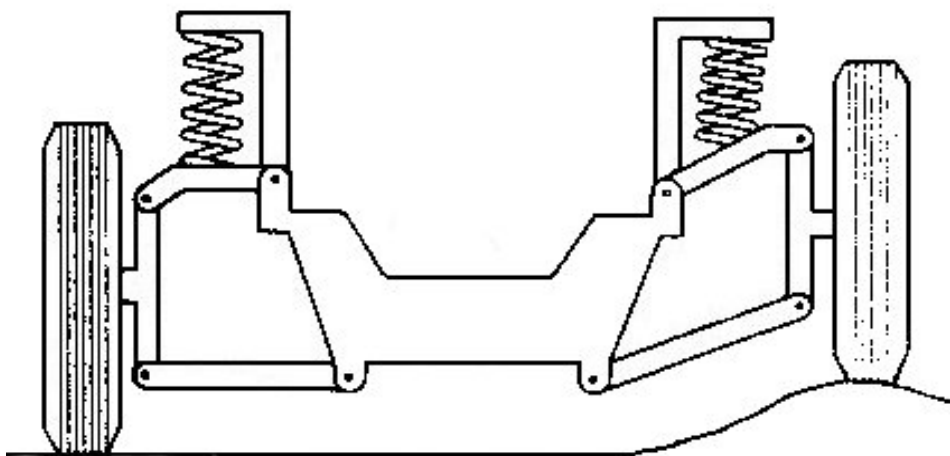
Figure 2.2. A second type of independent front suspension system
(Source: Remling 1983)
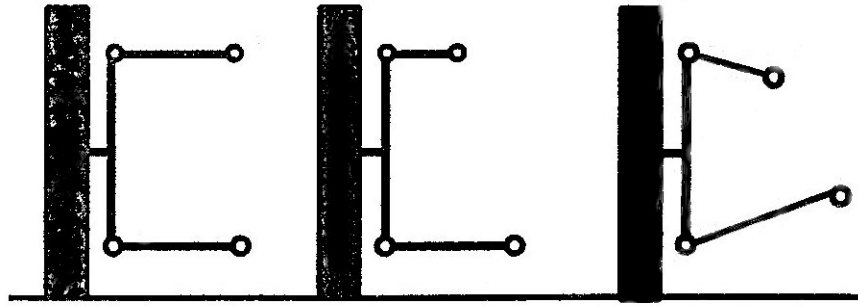
(a) Parallel and equal   (b) Parallel and unequal   (c) Nonparallel and unequal
Figure 2.3. Double wishbone suspension designs
(Source: Ünlüsoy 2000)

2.3. Vehicle Dynamics

The subject of "vehicle dynamics" is concerned with the movements of vehicles "automobiles, trucks, buses and special-purpose vehicles" on a road surface. The movements of interest are acceleration and braking, and turning or cornering. Dynamic behaviour is determined by the forces imposed on the vehicle from the tires, gravity, and aerodynamics. The vehicle and its components shall be studied to determine what forces will be produced by each of these sources at a particular maneuver and trim condition, and how the vehicle will respond to these forces. For that purpose, it is essential to establish a rigorous approach to modelling the vehicle and conventions that will be used to describe motions. The basic vehicle model and its parameters are given in Figure 2.4 and Table 2.1.
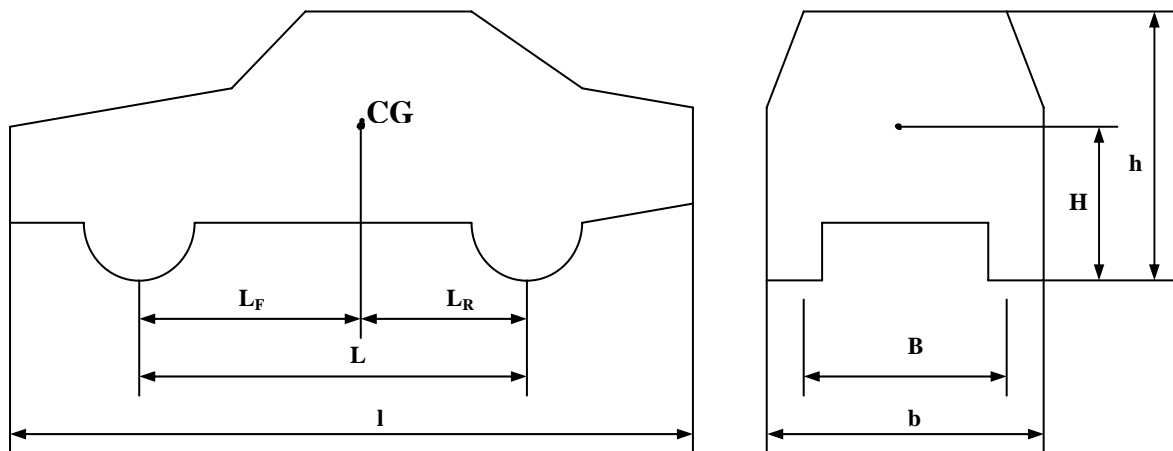
Figure 2.4. Basic vehicle model

7

Table 2.1. Description of parameters for the basic vehicle model

Parameters	Descriptions
b	Width of vehicle
B	Front axle track width
h	Height of vehicle
H	Height of center of gravity
l	Length of vehicle
L	Wheelbase
L_F	Distance from front axle to CG
L_R	Distance from rear axle to CG

2.3.1. Static Axle Loads
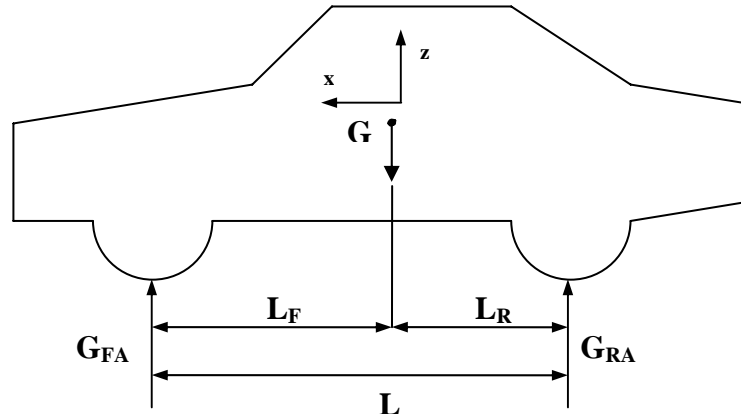
Figure 2.5. Static axle loads on the vehicle

Consider the vehicle shown in Figure 2.5. The weight of vehicle acting at its centre of gravity is:

$$G = m \cdot g \tag{2.1}$$

The loads on the front and rear axles are found by using the equilibrium equations;

$$G_{FA} = G.\frac{L_R}{L} \tag{2.2}$$

$$G_{RA} = G.\frac{L_F}{L} \tag{2.3}$$

Static load on one wheel of the front axle is:

$$G_{FAw} = \frac{G_{FA}}{2} \tag{2.4}$$

2.3.2. Dynamic Axle Loads

Dynamic behaviour is determined by the forces imposed on the vehicle from the tires, gravity and aerodynamics. In a real car, the wheel loads are constantly changing. These loads may be in the longitudinal direction such as acceleration and braking forces, in the lateral direction such as cornering forces, and in the vertical direction. In order to demonstrate how wheel loads can be calculated, a number of operational and simplifying assumptions are made.

Preliminary analysis is done assuming steady state operating conditions. The assumptions are smooth road way, constant speed cornering, constant longitudinal acceleration, constant grade. All calculations presented are based on the main assumption that the chassis of the car under consideration is rigid.

Calculation of the loads at each wheel in different operating conditions will be discussed for the rest of this section:

♦ The vehicle braking on level ground (Longitudinal weight transfer)
♦ The vehicle at the instant of cornering (Lateral load transfer on banking)
♦ The vehicle on a downhill grade
♦ The vehicle at the instant of braking on a downhill grade

Case 1 : The Vehicle Braking on Level Ground
(Longitudinal Weight Transfer)

Figure 2.6. Forces acting on a vehicle during braking

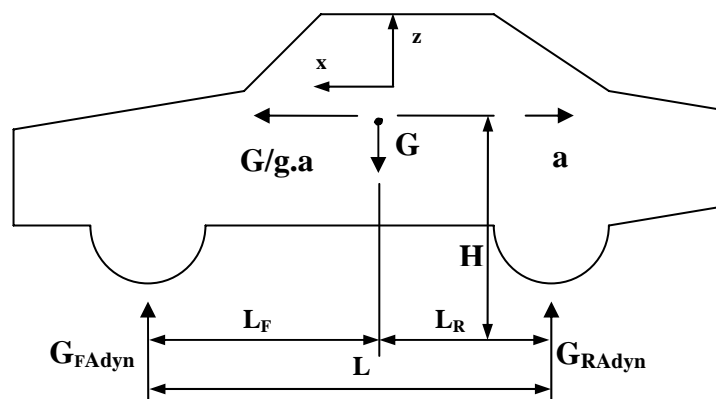The car is under negative acceleration as shown in Figure 2.6, an inertial reaction force denoted by (G/g.a) acting at the centre of gravity opposite to the direction of the acceleration. During the vehicle decelerates, load is transferred from the rear axle to the front axle.

By considering the equilibrium of moments about the front and rear tire-ground contact points, the normal loads on the front and rear axles are:

$$G_{FAdyn} = \frac{G.L_R + m.a.H}{L} \tag{2.5}$$

$$G_{RAdyn} = \frac{G.L_F - m.a.H}{L} \tag{2.6}$$

The transferred load to the front axle is found from the following equation:

$$G_T = G_{FAdyn} - G_{FA} \tag{2.7}$$

Case 2 : The Vehicle at the instant of Cornering
(Lateral Load Transfer on Banking)

When a car in a steady state turn with constant speed on banking as shown in Figure 2.7, load is transferred from the inside to the outside pair of wheels. During the steady-state turn an inertial reaction force called centrifugal force is developed which opposes the lateral acceleration produced by tire cornering forces. The cornering force produced by the tires, $S_L + S_R$, results in a lateral acceleration.

The centrifugal force which results from the speed V, the radius of the bend R and the total weight of the vehicle is;

$$F_c = \frac{m.V^2}{R} \tag{2.8}$$

During the turning, tires are required to produce longitudinal or side forces to hold the vehicle in the desired turn. The cornering force produced by the tires:

$$S = S_L + S_R = f_s.G = f_s(G_{LSdyn} + G_{RSdyn}) \tag{2.9}$$

where f_s is the friction coefficient between the road and tire.

The dynamic axle loads are found by using the moment equilibriums;

$$G_{RSdyn} = \frac{G}{B} \left[\frac{V^2}{g.R} \left(H.\cos\beta + \frac{B}{2}.\sin\beta \right) + \frac{B}{2}.\cos\beta - H.\sin\beta \right] \tag{2.10}$$

$$G_{LSdyn} = \frac{G}{B} \cdot \left[\frac{V^2}{g.R} \cdot \left(\frac{B}{2} . \sin\beta - H. \cos\beta \right) + \frac{B}{2} . \cos\beta + H. \sin\beta \right] \qquad (2.11)$$

Transferred load from the left side to the right side of the vehicle while cornering;

$$G_C = G_{RSdyn} - \frac{G}{2} \qquad (2.12)$$

(Milliken F. and Milliken L., 1995)
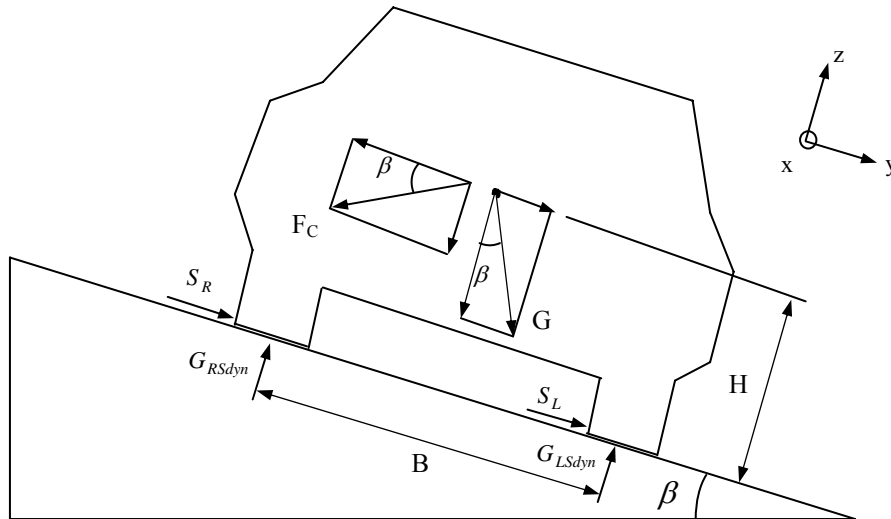
Figure 2.7. Forces acting on a vehicle during cornering

Case 3 : The Vehicle on a Downhill Grade

A negative grade causes load to be transferred from the rear to the front axle. On roads, the grade angle occasionally reaches 10 to 12 percent.

The major external forces acting on a two axle vehicle are shown in Figure 2.8. In the longitudinal direction, the aerodynamic resistance R_a, rolling resistance of the front and rear tires R_{rf} and R_{rr} are neglected for this case.

The dynamic loads on the front and rear axle are determined by summing moments equilibriums;

$$G_{FAdyn} = \frac{G}{L} \cdot (H.\mathrm{Sin}\alpha + L_R . \mathrm{Cos}\alpha) \qquad (2.13)$$

$$G_{RAdyn} = \frac{G}{L} \cdot (L_F . \mathrm{Cos}\alpha - H.\mathrm{Sin}\alpha) \qquad (2.14)$$
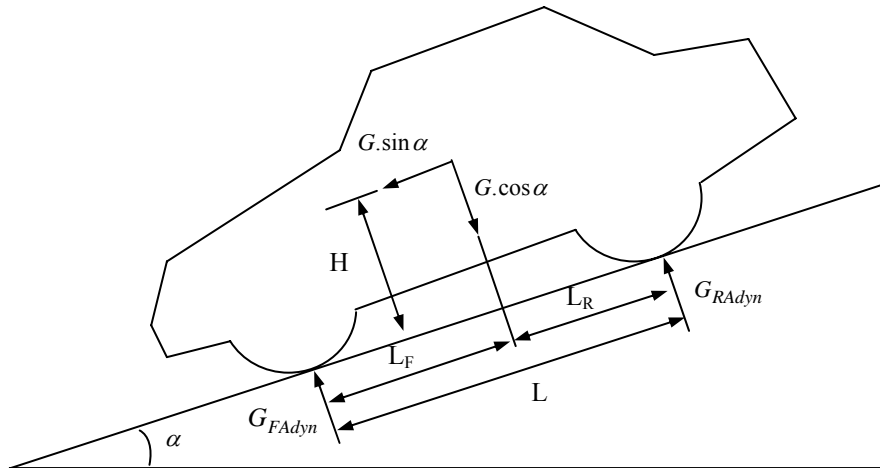
Figure 2.8. Forces acting on a vehicle on a downhill grade

Transferred load from rear axle to front axle is:

$$G_T = G_{FAdyn} - G_{FA} \qquad (2.15)$$

Case 4 : The Vehicle at the instant of Braking on a Downhill Grade

The effects of grade and longitudinal negative acceleration (braking) can be combined in finding the changes in front and rear loads. The external forces acting on a decelerating vehicle is shown in Figure 2.9. In addition to the braking force, rolling resistance of tires, aerodynamic resistance and transmission resistance also affect vehicle motion during braking are considered for this case.
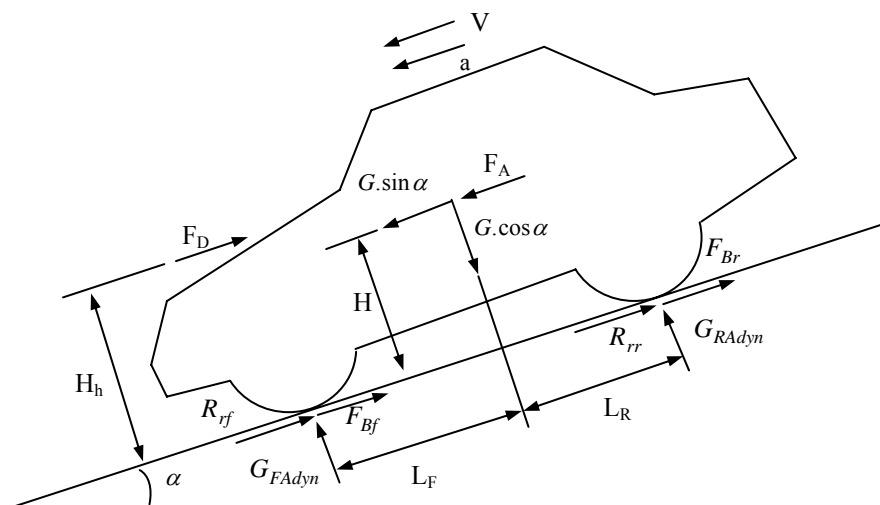
Figure 2.9. Forces acting on a vehicle braking on a downhill grade

The dynamic loads on the front and rear axle are determined by summing moments equilibriums;

$$G_{FAyin} = \frac{1}{L}[G.(H.\sin\alpha + L_R.\cos\alpha) + F_A.H - F_D.H_h]$$ (2.16)

$$G_{RAdyn} = \frac{1}{L}[G.(L_F.\cos\alpha - H.\sin\alpha) + F_D.H_h - F_A.H]$$ (2.17)

The braking inertia force is:

$$F_A = m.a$$ (2.18)

The aerodynamic forces produced on a vehicle arise from two sources; form (or pressure) drag and rolling resistance of the tires. Drag is the largest and most important aerodynamic force. The aerodynamic drag is:

$$F_D = c_D.A.\frac{\rho_a}{2}.V^2$$ (2.19)

The drag coefficient, c_D, is determined empirically for the car. The frontal area, A is the scale factor taking into account the size of the car. The frontal area of the vehicle in range of 79-84% of area calculated from the overall vehicle width and height. The frontal area %80 of area is:

$$A = 0,80.b.h$$ (2.20)

The aerodynamic force is assumed to be acting on the centre of the vehicle cross-section area:

$$H_h = \frac{h}{2}$$ (2.21)

The other major vehicle resistance force on level ground is the rolling resistance of the tires by the equation;

$$F_R = G.f_R.\cos\alpha$$ (2.22)

By considering the force equilibrium in the horizontal direction, the following relationship is established;

$$F_B = F_{Bf} + F_{Br} = f_s.(G_{FAdyn} + G_{RAdyn}) = m.a - F_R - F_D + G.\sin\alpha$$ (2.23)

where F_{Bf} and F_{Br} are the braking forces of the front and rear axles, respectively. The magnitude of the transmission resistance is small and can be neglected in the braking calculations (Wong 1993, Gillespie 1992).

2.4. Kinetic Analysis of Double Wishbone Suspension

In this section, the forces on the double wishbone suspension system are given. The maximum force G_{dyn} and lateral force S_{dyn} at the centre of the front axle tyre contact for the vehicle braking and cornering on a downhill grade are defined. The forces B_x and B_y are on the joint B of the lower suspension and A_x and A_y are on the joint A of the upper suspension control arm.

The loads on the A and B joints are found by summing moments about points "A" and "B". The moment equilibrium; $\sum M_B = 0$;

$$A_x.c + A_y.(a - b) = G_{din}.b + S_{din}.d \tag{2.24}$$

where $A_x = F_A.\cos\delta$ and $A_y = F_A.\sin\delta$, in which F_A is the force acting on the link AE. The force equilibriums in the direction x and y;

$$B_x = S_{dyn} + A_x \tag{2.25}$$

$$B_y = G_{dyn} - A_y \tag{2.26}$$

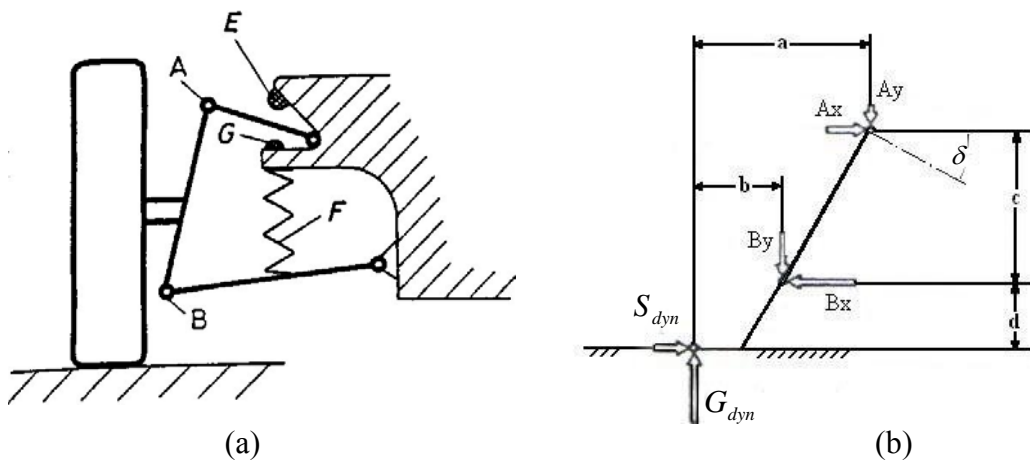(Reimpell 1973)

<div align="center">(a)   (b)</div>

Figure 2.10. Double wishbone suspension system: (a) Kinematic model of double wishbone suspension (b) Forces on the lower and upper arms (Source: Reimpell 1973)

CHAPTER 3

MODELLING AND DYNAMIC ANALYSIS

3.1. Introduction to Finite Element

In Finite Element Method, a complex region defining a continuum is discretized into simple geometric shapes called finite elements. The material properties and the governing relationships are considered over these elements and expressed in terms of unknown values at the nodes. An assembly process, duly considering the loading and constraints, results in a set of equations. Solution of these equations gives us approximate behaviour of the continuum (Belegundu and Chandrupatla 1997).

In this chapter, use of the analytical method and finite element method for the dynamic analysis of double wishbone suspension system is described. Mass, stiffness and geometric stiffness matrices are derived. The plane frame element is selected to model the double wishbone suspension members.

3.2. Characteristic Matrices of the Plane Frame Element

A planar (2-D) frame element is subjected to both axial and bending deformations. Therefore, the plane frame element has three degrees of freedom per node together with local displacements (u_1, v_1 and θ_1) and global displacements ($\bar{u}_1$, $\bar{v}_1$ and $\bar{\theta}_1$) as shown in Figure 3.1. The nodal displacement vector is given by;

$$\{q\} = \{u_1, v_1, \theta_1, u_2, v_2, \theta_2\}^T \tag{3.1}$$

The element stiffness matrix for a 2-D frame element can be constructed by superimposing both axial and bending stiffness (Bang and Kwon 1997).

The element kinetic and strain energy functions for plane frame element are given in terms of local coordinates, as follows;

$$T = \frac{1}{2} \int_e \rho A (\dot{u}^2 + \dot{v}^2) \ dx \tag{3.2}$$

where the overdot shows the differentiation with respect to time.
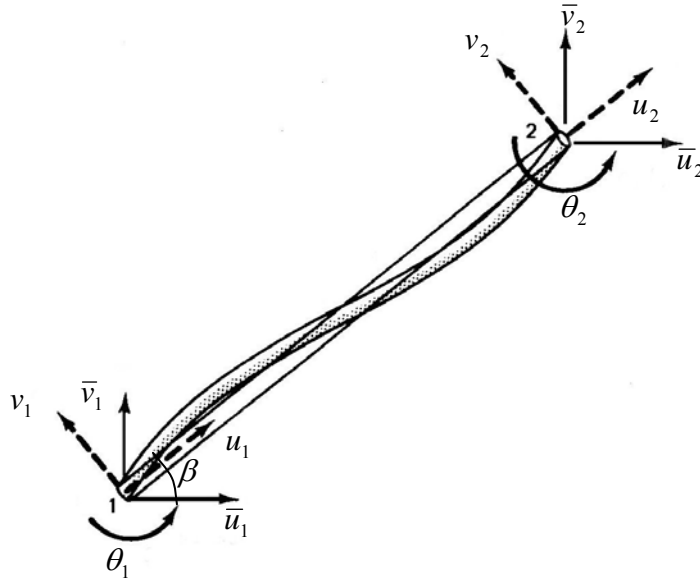
Figure 3.1. Plane frame element
(Source: Belegundu and Chandrupatla 1997)

$$U = \frac{1}{2} \int_e EA(\frac{\partial u}{\partial x})^2 \; dx + \frac{1}{2} \int_e EI(\frac{\partial^2 v}{\partial x^2})^2 \; dx \qquad (3.3)$$

In these expressions, u and v are the axial and transverse displacement respectively. The displacement functions are;

$$u = [N_u(\xi)] \; \{u\}_e \qquad\qquad (3.4a)$$

$$v = [N_v(\xi)] \; \{v\}_e \qquad\qquad (3.4b)$$

The subscripts u and v are introduced here to differentiate between axial and transverse displacements. $[N_i(\xi)]$ represents the shape functions. The detail explanations of shape functions can be found in references (Petyt 1990, Belegundu and Chandrupatla 1997).

3.2.1. Elastic Stiffness Matrix

Substituting the displacement functions given in Equation (3.4) into the strain energy expression given in Equation (3.3) gives,

$$U_e = \frac{1}{2} \{u\}_e^T [\tilde{k}]_e \{u\}_e \qquad\qquad (3.5)$$

16

where

$$[\tilde{k}]_e = \frac{EI_z}{2a^3} \begin{bmatrix} (a/r_z)^2 & 0 & 0 & -(a/r_z)^2 & 0 & 0 \\ 0 & 3 & 3a & 0 & -3 & 3a \\ 0 & 3a & 4a^2 & 0 & -3a & 2a^2 \\ -(a/r_z)^2 & 0 & 0 & (a/r_z)^2 & 0 & 0 \\ 0 & -3 & -3a & 0 & 3 & -3a \\ 0 & 3a & 2a^2 & 0 & -3a & 4a^2 \end{bmatrix} \tag{3.6}$$

in which $\ell_e = 2a$ and $r_z{}^2 = I_z / A$ (Petyt 1990).

3.2.2. Geometric Stiffness Matrix

The geometric strain energy in the element is;

$$U_g = \int_0^L \frac{P}{2}\left(\frac{\partial v}{\partial x}\right)^2 dx = \frac{1}{2}\{q\}^T [\tilde{s}]_e \{q\} \tag{3.7}$$

The geometric stiffness matrix $[\tilde{s}]$ for a plane frame is developed from the Equation (3.7);

$$[\tilde{s}]_e = \frac{P}{60a} \begin{bmatrix} 0 & 0 & 0 & 0 & 0 & 0 \\ 0 & 36 & 6a & 0 & -36 & 6a \\ 0 & 6a & 16a^2 & 0 & -6a & -4a^2 \\ 0 & 0 & 0 & 0 & 0 & 0 \\ 0 & -36 & -6a & 0 & 36 & -6a \\ 0 & 6a & -4a^2 & 0 & -6a & 16a^2 \end{bmatrix} \tag{3.8}$$

where $\ell_e = 2a$ and P is the axial force, (Cook, Malkus and Plesha 1989).

3.2.3. Mass Matrix

Substituting the displacement functions given in Equation (3.4) into the kinetic energy expression given in Equation (3.2) gives;

$$T = \frac{1}{2}\{\dot{u}\}_e{}^T [\tilde{m}]_e \{\dot{u}\}_e \tag{3.9}$$

where

$$[\widetilde{m}]_e = \frac{\rho A a}{105} \begin{bmatrix} 70 & 0 & 0 & 35 & 0 & 0 \\ 0 & 78 & 22a & 0 & 27 & -13a \\ 0 & 22a & 8a^2 & 0 & 13a & -6a^2 \\ 35 & 0 & 0 & 70 & 0 & 0 \\ 0 & 27 & 13a & 0 & 78 & -22a \\ 0 & -13a & -6a^2 & 0 & -22a & 8a^2 \end{bmatrix} \qquad (3.10)$$

in which $\ell_e = 2a$, ρ is the mass per unit volume, and A is the cross-sectional area of each element (Petyt 1990).

3.2.4. Stiffness of the Spring

In finite element model, stiffness of helical-shaped springs used in suspension system may be expressed in matrix notation considering the plane frame element displacement vector as follows;

$$[\widetilde{k}_s] = k \begin{bmatrix} 0 & 0 & 0 & 0 & 0 & 0 \\ 0 & 1 & 0 & 0 & -1 & 0 \\ 0 & 0 & 0 & 0 & 0 & 0 \\ 0 & 0 & 0 & 0 & 0 & 0 \\ 0 & -1 & 0 & 0 & 1 & 0 \\ 0 & 0 & 0 & 0 & 0 & 0 \end{bmatrix} \qquad (3.11)$$

where k is the stiffness coefficient of the spring by the equation;

$$k = \frac{G_s d^4}{64 n R_s^{\,3}} \qquad (3.12)$$

The stiffness is a function of the shear modulus (G_s), the diameter of the turns of coils (R_s), the diameter of the coils (d), and the number of the coils (n) (Inman 1996).

3.2.5. Coordinate Transformation

If a frame member is inclined in global coordinate system as shown in Figure 3.1, the element stiffness, mass and geometric stiffness matrices require the planar transformation. Figure 3.1 shows the nodal freedoms in local and global systems.

The relation between the local and global displacements is;

$$
\begin{Bmatrix} u_1 \\ v_1 \\ \theta_1 \\ u_2 \\ v_2 \\ \theta_2 \end{Bmatrix} = \begin{bmatrix} c & s & 0 & 0 & 0 & 0 \\ -s & c & 0 & 0 & 0 & 0 \\ 0 & 0 & 1 & 0 & 0 & 0 \\ 0 & 0 & 0 & c & s & 0 \\ 0 & 0 & 0 & -s & c & 0 \\ 0 & 0 & 0 & 0 & 0 & 1 \end{bmatrix} \begin{Bmatrix} \bar{u}_1 \\ \bar{v}_1 \\ \theta_1 \\ \bar{u}_2 \\ \bar{v}_2 \\ \theta_2 \end{Bmatrix}
\tag{3.13}
$$

where $c = \cos\beta$ and $s = \sin\beta$.

In the short notation, Equation (3.13) can be written as;

$$\{u\}_e = [R]_e\{\bar{u}\}_e \tag{3.14}$$

Substituting Equation (3.14) into the energy expressions given in Equations (3.2) and (3.3) gives,

$$T = \frac{1}{2}\{\bar{u}\}_e{}^T[m]_e\{\bar{u}\}_e \tag{3.15}$$

$$U_e = \frac{1}{2}\{\bar{u}\}_e{}^T[k]_e\{\bar{u}\}_e \tag{3.16}$$

$$U_g = \frac{1}{2}\{\bar{u}\}_e{}^T[s]_e\{\bar{u}\}_e \tag{3.17}$$

The stiffness and mass matrices for a planar frame element are expressed in terms of the global coordinate system as given below,

$$[M]_e = [R]_e{}^T[\tilde{m}]_e[R]_e \tag{3.18}$$

$$[K]_e = [R]_e{}^T[\tilde{k}]_e[R]_e \tag{3.19}$$

$$[S]_e = [R]_e{}^T[\tilde{s}]_e[R]_e \tag{3.20}$$

(Kwon and Bang 1997, Petyt 1990).

3.3. Modelling of Double Wishbone Suspension

3.3.1. Modelling Assumptions

Figure 3.2 shows a part of a chassis with a double wishbone suspension system. The mechanical system consists of a main chassis, a double wishbone suspension sub-system and a wheel. A suspension spring, lower and upper arms are included in the suspension sub-system. The lower and upper arms are modelled by simple links.

The chassis is constrained to move vertically upward or downward. The wheel can be modelled as a linear translational spring. The motion of the wheel over the road provides a vertical input which excites the body of the vehicle.

The quarter car with the double wishbone suspension is modelled depending on two different assumptions due to the suspension links. In the first model, the links of the suspension are assumed to be rigid links. In the second model, finite element model, links are modelled to be flexible.
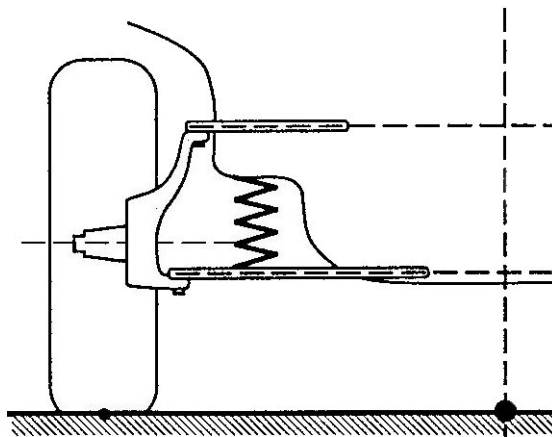

Figure 3.2. A quarter car with the double wishbone suspension
(Source:Gillespie 1992)

For analysis purpose, the model of the quarter car with the double wishbone suspension assumed to travel with constant velocity on a road surface characterized by a displacement $y_g(t)$. Angular displacements of the lower and upper links are negligible since the amplitude of the base displacement (amplitude of $y_g(t)$) is chosen in small amplitude. On the other hand, in order to have the linear equation of motion, axial link forces are assumed as constant.

3.3.2. Simple Modelling of Suspension System

Double wishbone suspension of a quarter car is modelled assuming the suspension links to be rigid. The model is shown in Figure 3.3.

The mass m_t represents approximately the mass of the wheel plus part of the mass of the suspension arms, m_c represents approximately 1/4 of the car mass.

The excitation comes from the road irregularity. It is considered that the spring is located in the middle of the lower control arm.

The kinetic and strain energies;

$$T = \frac{1}{2}m_c\dot{v}_1^2 + \frac{1}{2}m_t\dot{v}_3^2 = \frac{1}{2}\{\dot{q}\}^T[M]\{\dot{q}\} \tag{3.21}$$

$$U = \frac{1}{2}k_t\left(y_g - v_3\right)^2 + \frac{1}{2}k(v_2 - v_1)^2 = \frac{1}{2}\{q\}^T[K]\{q\} \tag{3.22}$$
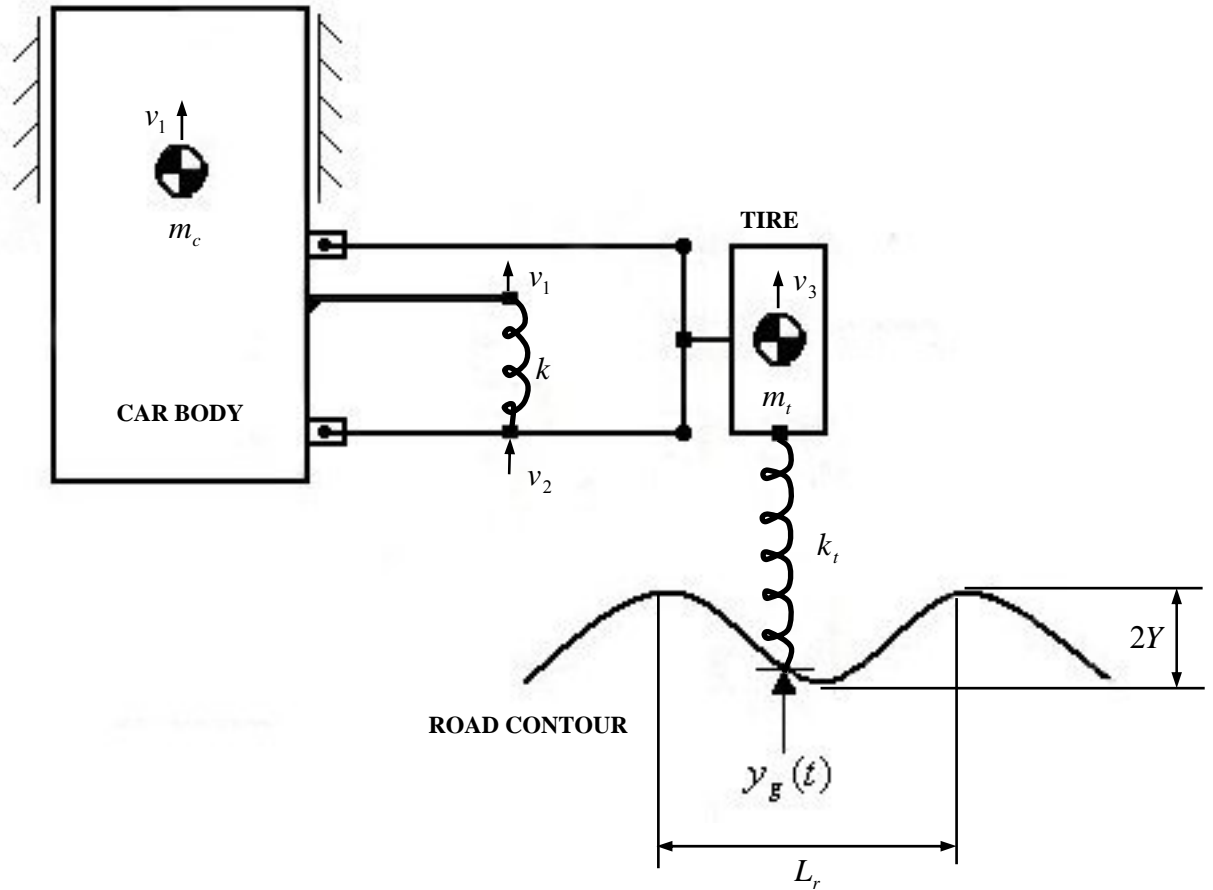
Figure 3.3. Simple model of the suspension system

The Lagrange's equations;

$$\frac{d}{dt}\left(\frac{\partial T}{\partial \dot{q}_i}\right) + \frac{\partial U}{\partial q_i} = Q_i \qquad\qquad i = 1,2,...........n \tag{3.23}$$

where the total strain energy $U = U_e + U_g$, and Q_i are generalised forces.

The Lagrange's equations (3.23) yield the equations of motions in matrix form to find the natural frequencies;

$$[M]\{\ddot{q}\} + [K]\{q\} = \{Q\} \tag{3.24}$$

The equation (3.23) can be written for v_1;

$$\frac{d}{dt}\left(\frac{\partial T}{\partial \dot{v}_1}\right) + \frac{\partial U}{\partial v_1} = Q_1 \tag{3.25}$$

$$v_2 = \frac{(v_1 + v_3)}{2} \tag{3.26}$$

$$m_c \ddot{v}_1 + k\left(\frac{v_1 - v_3}{4}\right) = 0 \tag{3.27}$$

The equation (3.23) can be written for v_3;

$$\frac{d}{dt}\left(\frac{\partial T}{\partial \dot{v}_3}\right) + \frac{\partial U}{\partial v_3} = Q_2 \tag{3.28}$$

$$m_t \ddot{v}_3 + k_t\left(v_3 - y_g\right) + k\left(\frac{v_3 - v_1}{4}\right) = 0 \tag{3.29}$$

The differential equations in matrix form are;

$$\begin{bmatrix} m_c & 0 \\ 0 & m_t \end{bmatrix}\begin{Bmatrix} \ddot{v}_1 \\ \ddot{v}_3 \end{Bmatrix} + \begin{bmatrix} k/4 & -k/4 \\ -k/4 & (k/4) + k_t \end{bmatrix}\begin{Bmatrix} v_1 \\ v_3 \end{Bmatrix} = \begin{Bmatrix} 0 \\ k_t y_g \end{Bmatrix} \tag{3.30}$$

The system characteristic matrices are;

$$[M] = \begin{bmatrix} m_c & 0 \\ 0 & m_t \end{bmatrix} \tag{3.31}$$

$$[K] = \begin{bmatrix} k/4 & -k/4 \\ -k/4 & (k/4) + k_t \end{bmatrix} \tag{3.32}$$

The generalized force vector is;

$$\{Q\} = \begin{Bmatrix} 0 \\ k_t y_g(t) \end{Bmatrix} \tag{3.33}$$

On the other hand, Equation (3.30) represents a mathematical model shown in Figure 3.4.

If the base displacement is defined by a single frequency harmonic of the form as, $y_g(t) = Y.Sinw_e t$. The frequency of base motion, w_e, is;

$$w_e = \frac{2\pi V}{L_r} \tag{3.34}$$

where V is the vehicle speed and L_r is the period of the road profile.
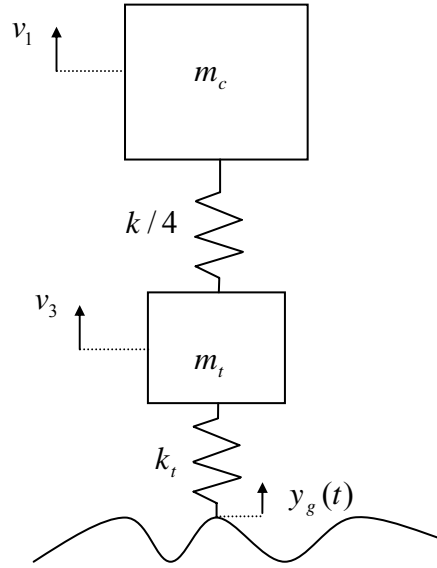
Figure 3.4. A quarter car suspension model
(Source:Gobbi and Mastinug 2001)

3.3.3. Finite Element Modelling of Suspension System

The lower and the upper arms are divided into two elements, as shown in Figure 3.5. The degrees of freedom of node i are u_i, v_i and θ_i. The degree of freedom v_i is transverse displacement and u_i is axial displacement and θ_i is slope or rotation.

The global displacement vector;

$$\{q\} = \{u_1, v_1, \theta_1, u_2, v_2, \theta_2, u_3, v_3, \theta_3, u_4, \theta_4, u_5, v_4, \theta_5, \theta_6, \theta_7\}^T \tag{3.35}$$

The local degrees of freedom for a single element are represented by Equation (3.1);

$$\{q_e\} = \{u_1, v_1, \theta_1, u_2, v_2, \theta_2\}^T$$

The connectivity table for the element solution is given in Table 3.1. Every node in an element has both a local coordinate and a global coordinate. The elastic stiffness, geometric stiffness, mass matrices are found from Equations (3.6), (3.8), and (3.10) for each the plane frame element. The global stiffness, geometric, and mass matrices are obtained by assembling these element matrices. The spring element given in Equation (3.12) is considered a frame element.

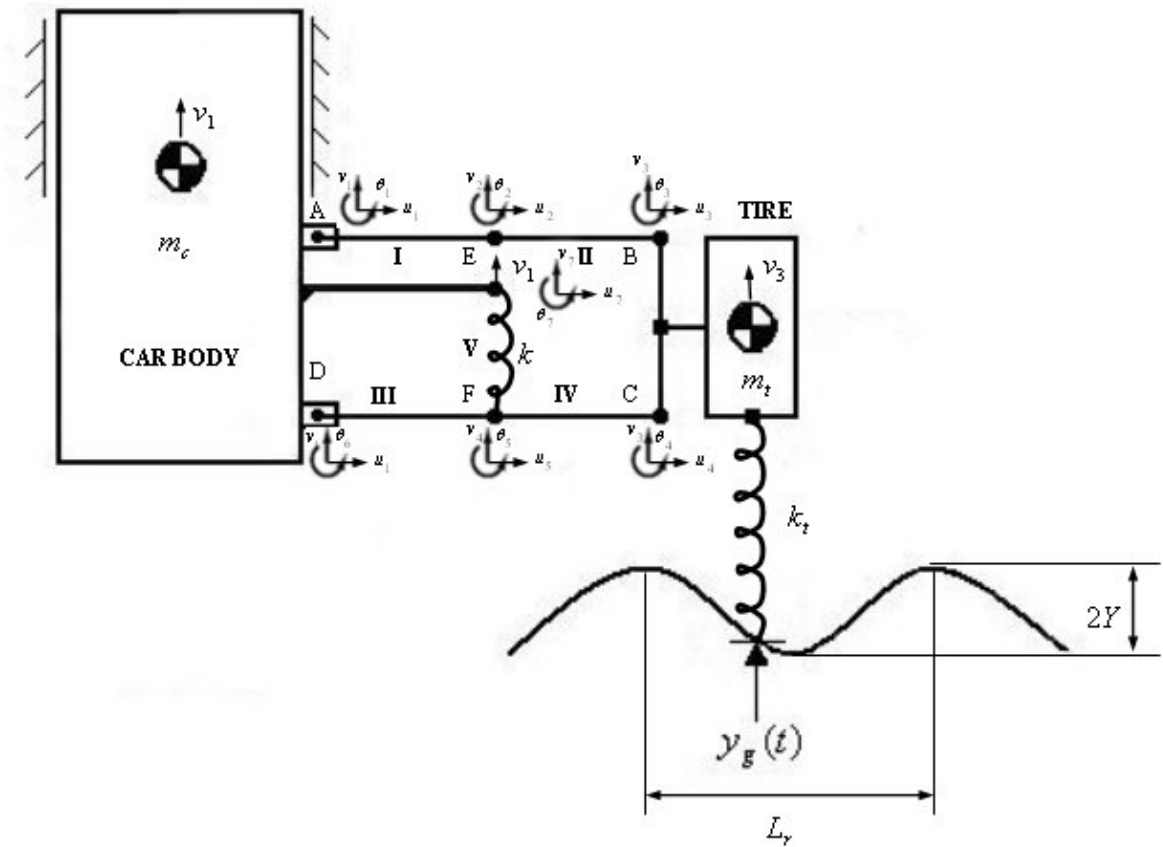Figure 3.5. Finite element model of the suspension system

Table 3.1. Global freedom numbers for the finite element model

Element Number	Local Freedom Numbers					
	1	2	3	4	5	6
I	1	2	3	4	5	6
II	4	5	6	7	8	9
III	1	2	15	12	13	14
IV	12	13	14	10	8	11
V	12	13	14	1	2	16

3.3.4. Proportional Damping

For the sake of simplicity, proportional damping is employed to find the time response of the system. Proportional damping matrix is given by;

$$[C] = a_1 [M] + a_2 [K]$$ (3.36)

where a_1 and a_2 are proportional damping coefficients.

The damping ratio for the nth mode of such a system is:

$$\xi_n = \frac{a_1}{2}\frac{1}{w_n} + \frac{a_2}{2}w_n$$ (3.37)

The coefficients a_1 and a_2 can be determined from specified damping ratio ξ_i and ξ_j for the ith and jth modes, respectively. Expressing Equation (3.37) for these two modes in matrix form leads to

$$\frac{1}{2}\begin{bmatrix} 1/w_i & w_i \\ 1/w_j & w_j \end{bmatrix}\begin{Bmatrix} a_1 \\ a_2 \end{Bmatrix} = \begin{Bmatrix} \xi_i \\ \xi_j \end{Bmatrix}$$ (3.38)

These two algebraic equations can be solved to determine the coefficients a_1 and a_2. If both modes are assumed to have the same damping ratio ξ, which is reasonable based on experimental data, then

$$a_1 = \xi\frac{2w_i w_j}{w_i + w_j} \qquad a_2 = \xi\frac{2}{w_i + w_j}$$ (3.39)

(Cook 1989, Chopra 1995).

3.4. The Equation of Motions of the Suspension System

The equation of motion considering the proportional damping after the assembly procedure takes the form;

$$[M]\{\ddot{q}\} + [C]\{\dot{q}\} + ([K] + [S])\{q\} = \{Q\}$$ (3.40)

where, $\{q\}$ is the column matrix of nodal displacements and $[C]$ is proportional damping matrix given in Equation (3.36). The method of solving Equation (3.40) depends upon whether the applied forces are harmonic, periodic, transient or random.

3.5. Vibrations of the Double Wishbone Suspension System

3.5.1. Natural Frequencies

In order to obtain the natural frequencies, Equation (3.40) is reduced to general eigenvalue problem given below;

$$(([K]+[S]) - w^2[M]).\{q\} = 0 \qquad (3.41)$$

where $[K]$, $[S]$ and $[M]$ are the global elastic stiffness, geometric stiffness, and mass matrices, respectively, and $\{q\}$ is global displacement vector. The eigenvalue problem is then solved by Matlab programs developed for two different models.

3.5.2. Response to Base Excitation

When a structure moves with the time under prescribed loads and motions of its supports; that is asked for a time-history analysis. Runge-Kutta integration method of time-history analysis is used to the numerical solutions. Matlab has two different Runge-Kutta based simulations: ode23 and ode45. These are automatic step-size integration methods. The M-file ode23 uses a simple second- and third-order pair of formulas for medium accuracy and ode45 uses a fourth- and fifth-order pair for greater accuracy. The detail information can be found in reference (Inman 1996).

Equation (3.40) is rewritten considering the initial conditions subject to a force that is function of time as;

$$[M]\{\ddot{q}(t)\}+[C]\{\dot{q}(t)\}+([K]+[S])\{q(t)\} = \{Q(t)\} \qquad (3.42a)$$

$$\{q(0)\} = \{q_0\} \qquad \{\dot{q}(0)\} = \{\dot{q}_0\} \qquad (3.42b)$$

In order to use the ode functions in Matlab, Equation (3.42) is transformed to first order differential equation by defining two new vectors by $\{y_1\} = \{q\}$ and $\{y_2\} = \{\dot{q}\}$. Then multiplying Equation (3.42) by $[M]^{-1}$ yields the coupled first-order vector differential equations;

$$\{\dot{y}_1\} = \{y_2\}$$

$$\{\dot{y}_2\} = -[M]^{-1}([K]+[S])\{y_1\}-[M]^{-1}[C]\{y_2\}+[M]^{-1}\{Q\} \qquad (3.43)$$

with initial conditions $\{y_1(0)\} = \{q_0\}$ and $\{y_2(0)\} = \{\dot{q}_0\}$.

Equation (3.43) is written as the single first-order equation;

$$\{\dot{y}(t)\} = [A]\{y(t)\} + \{f(t)\} \qquad \{y(0)\} = \{y_0\} \qquad\qquad (3.44)$$

where

$$A = \begin{bmatrix} 0 & I \\ -[M]^{-1}([K]+[S]) & -[M]^{-1}[C] \end{bmatrix} \qquad\qquad (3.45)$$

and

$$\{y(t)\} = \begin{bmatrix} \{y_1(t)\} \\ \{y_2(t)\} \end{bmatrix} \qquad\qquad \{f(t)\} = \begin{bmatrix} 0 \\ [M]^{-1}\{Q(t)\} \end{bmatrix} \qquad\qquad (3.46)$$

$$\{y_0\} = \begin{bmatrix} \{y_1(0)\} \\ \{y_2(0)\} \end{bmatrix} = \begin{bmatrix} \{q_0\} \\ \{\dot{q}_0\} \end{bmatrix} \qquad\qquad (3.47)$$

Here $\{y(t)\}$ is the ($2nx1$) state vector, where the first $nx1$ elements correspond to the displacement $\{q(t)\}$ and the second $nx1$ elements correspond to the velocities $\{\dot{q}(t)\}$ (Inman 1996).

CHAPTER 4

NUMERICAL APPLICATIONS

4.1. Results of the Kinetic Analysis of the Double Wishbone Suspension

In this section, based on the procedure described Section 2.4, the kinetic analysis of a double wishbone suspension system is presented. The main purpose of this section is to provide the axial force of the suspension links. The numerical data corresponding to the typical vehicle model used in defining the loads are given in Table 4.1. These forces are necessary to find the geometric stiffness properties of these links. The dynamic loads of the typical vehicle model shown in Figure 2.4 are analyzed.

Table 4.1. Numerical data of a typical vehicle model

Parameters	Numerical data
b (mm)	1961
B (mm)	1670
f_s	0,6
G_{FA}/ G_{RA}	44/56
h (mm)	2220
H (mm)	1160
l (mm)	4800
L (mm)	2900
L_F (mm)	1624
L_R (mm)	1276
m (kg)	3050
R (m)	100
α (degree)	11
β (degree)	0

Loads on the Vehicle for Different Road Conditions

The minimum acceleration value "a" given in brake regulation 71/320/EEC (ECE R13) is used. Rolling resistance coefficient f_R = 0.015, aerodynamic drag coefficient c_D = 0.32, air density ρ =1.228 kg/m^3 are chosen for the passenger car from the reference (Gillespie 1992). Static axle loads are calculated as 13164 N (G_{FA}) and 16755 N (G_{RA}) for front and rear axle, respectively. The static load on one wheel of the front axle is 6582 N (G_{FAw}). Dynamic axle loads are given in Table 4.2 for a vehicle speed of 80 and 120 km/h.

Table 4.2. Dynamic loads on the front one wheel of the vehicle

Road conditions	Dynamic loads (N)	
	G_{dyn}	S_{dyn}
Braking and cornering on a downhill grade (Case 2 + Case 4) V=80 km/h	17162	9081
Braking and cornering on a downhill grade (Case 2 + Case 4) V=120 km/h	25992	13754

Forces on the Suspension System Model

The calculated values of the joint forces for two different vehicle speeds are given in Table 4.3 with the suspension link parameters (a, b, c, and d) shown in Figure 2.10(b).

Table 4.3. Forces on the double wishbone suspension
(a= 154.68, b= 96.68, c= 248.17, d=265.67, and $\delta = 0$)

Vehicle speed (km/h)	Force on joints (N)			
	A_x	A_y	B_x	B_y
80	2927	463	12009	16698
120	4434	702	18187	25290

4.2. Results of the Vibration Analysis of the Simple Model of the Suspension System

The physical properties of the suspension model in Figure 3.3 are given in Table 4.4.

Table 4.4. Data of the vehicle and suspension

Parameters	Value
m_c (kg)	750
m_t (kg)	50
k (N/mm)	340
k_t (N/mm)	235
ξ (-)	0.2

The spring stiffness value is found from Equation (3.12) by using the following data; d=21.2 mm, G_s= 8.273e+004 N/mm^2 (for steel spring), n= 6.25 and R_s=50 mm. The proportional damping coefficients a_1 and a_2 are found from Equation (3.39) as 3.236 and 0.0045, respectively.

4.2.1. Natural Frequencies

A Matlab program depending on Equation (3.41) along with Equations (3.31) and (3.32) is developed to find the natural frequencies of the simple model of the suspension. Using the numerical data given in Table 4.4, the natural frequencies are found as w_1 = 9.101 rad/s and w_2 = 80.190 rad/s.

4.2.2. Response to Base Excitation

The road profile is chosen as sinusoidal in cross section with parameters L_r = 6 m and Y = 0.02 m. For the two vehicle speeds of 80 km/h and 120 km/h; the excitation frequencies are determined from Equation (3.34) as w_{e1} = 23.272 rad/s and w_{e2} = 34.908 rad/s. Figures 4.1 and 4.2 depict the time variations of the vertical

displacements of the car body, tire axis and the road profile for two different conditions aforementioned. Also, Figures 4.3 and 4.4 show plot of the displacements, velocities, and accelerations of the car body versus time for the two different excitation frequencies.
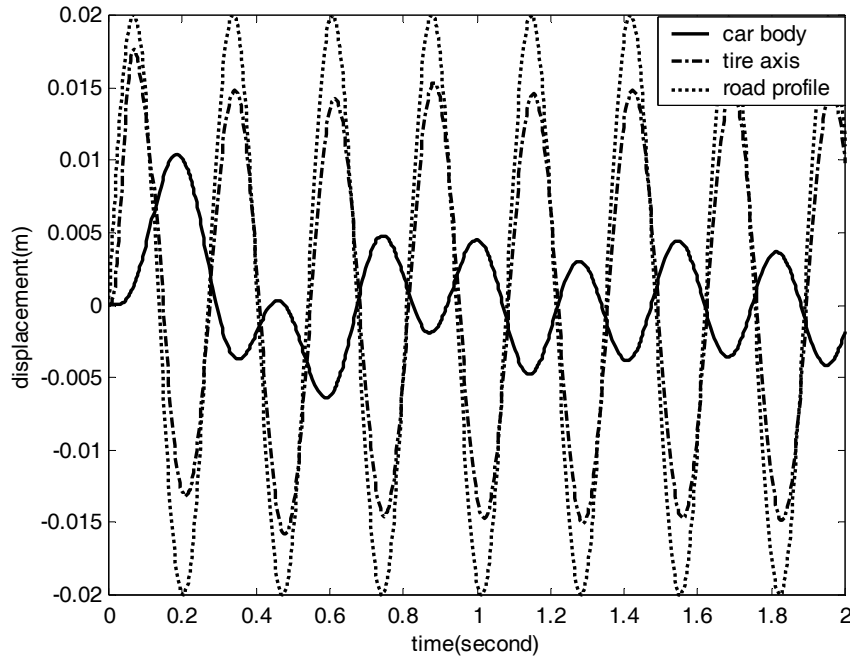

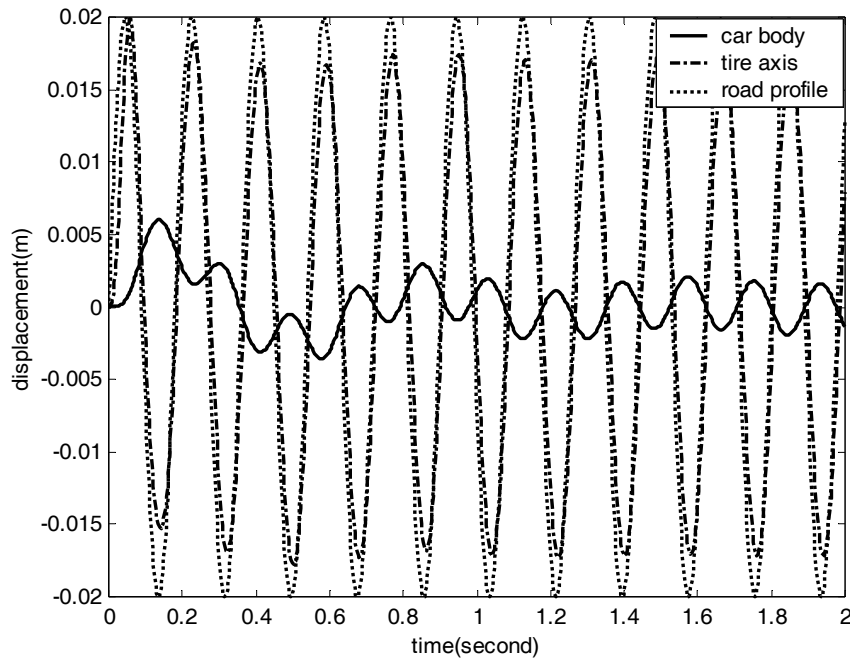Figure 4.1. Plot of the displacements vs time for simple model (V=80 km/h)

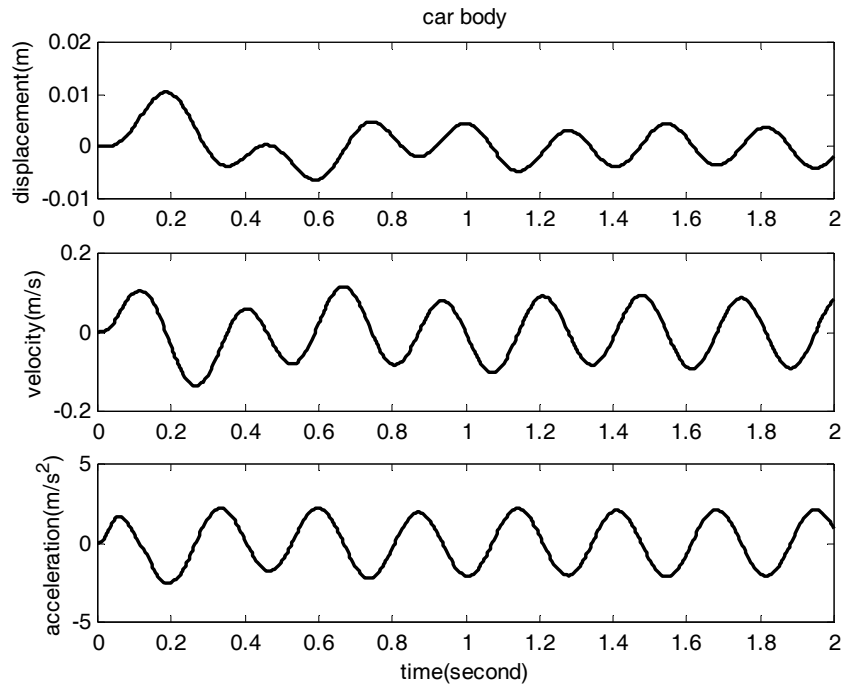Figure 4.2. Plot of the displacements vs time for simple model (V=120 km/h)

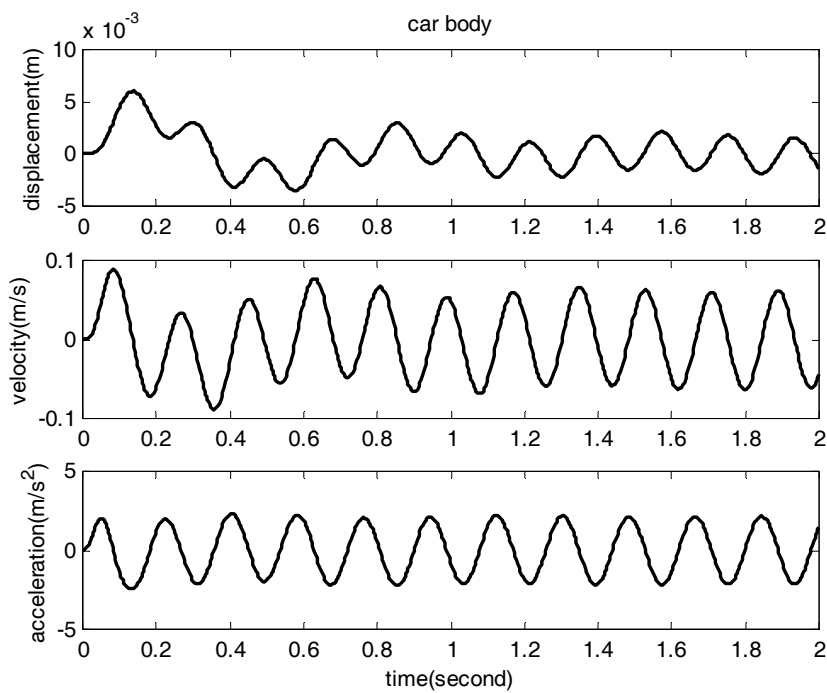Figure 4.3. Plot of the displacement, velocity, and acceleration vs time for simple model (V=80 km/h)

Figure 4.4. Plot of the displacement, velocity, and acceleration vs time for simple model (V=120 km/h)

4.3. Results of the Vibration Analysis of the Finite Element Model of the Suspension System

The physical properties of the suspension model in Figure 3.4 are given in Table 4.5.

Table 4.5. Numerical data for the finite element model

Parameters	Numerical Data
E (N/m^2)	2.1e+011
ρ (kg/m^3)	7830
$\ell_1, \ell_2, \ell_3, \ell_4$ (m)	0.2
A_1, A_2, A_3, A_4 (m^2)	6.0e-004
I_1, I_2, I_3, I_4 (m^4)	1.2e-007
ξ (-)	0.2

4.3.1. Natural Frequencies

A Matlab program depending on Equation (3.41) along with Equations (3.6), (3.8), (3.10), and (3.11) is developed to find the natural frequencies of the finite element model of the suspension. Using the numerical data given in Tables 4.4 and 4.5, the natural frequencies are found as $w_1 = 9.032$ rad/s and $w_2 = 79.043$ rad/s.

4.3.2. Response to Base Excitation

Similar investigations given in Section 4.2.2 are carried out for finite element model of the suspension system and the results are presented in Figures 4.5-4.8.
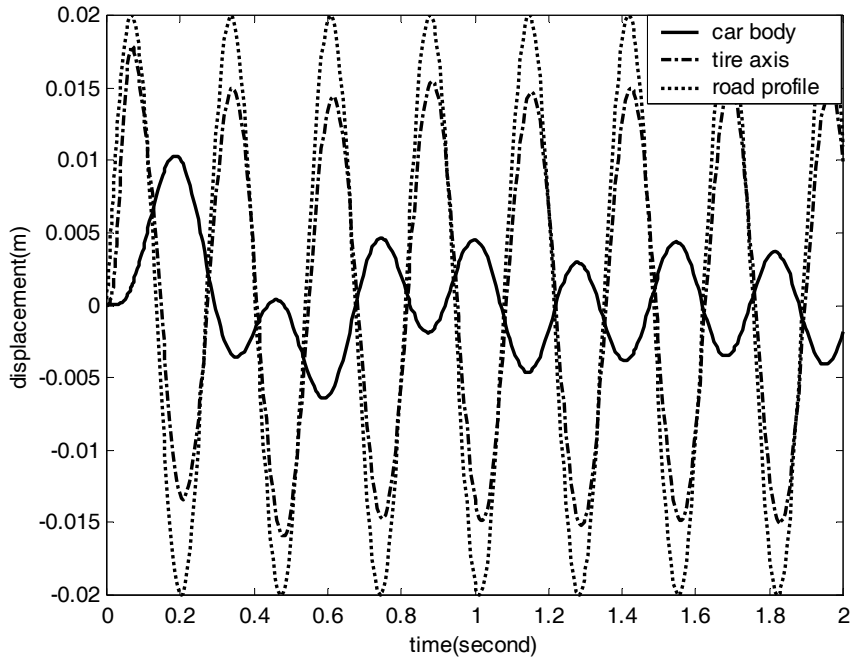
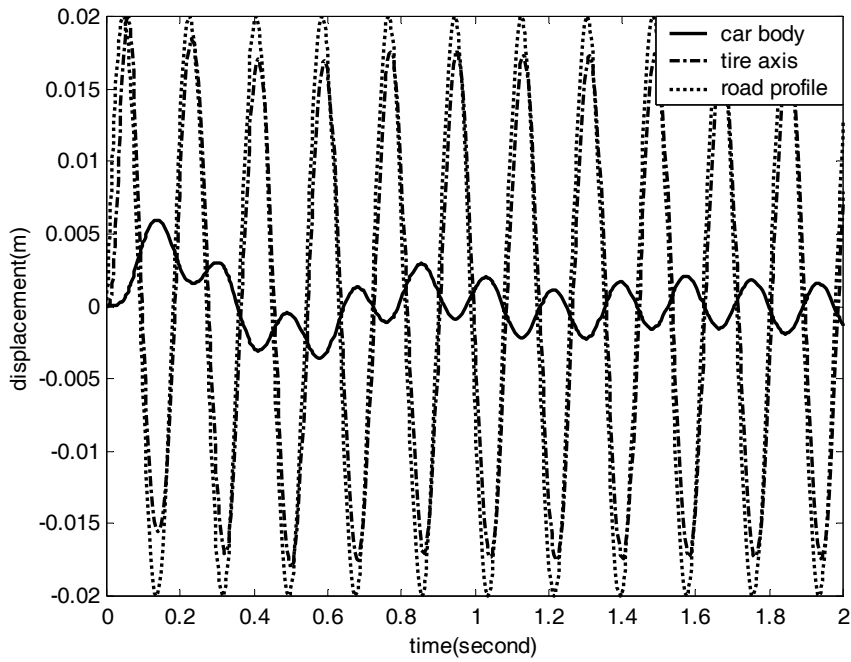Figure 4.5. Plot of the displacements vs time for unloaded FE model (V=80 km/h)

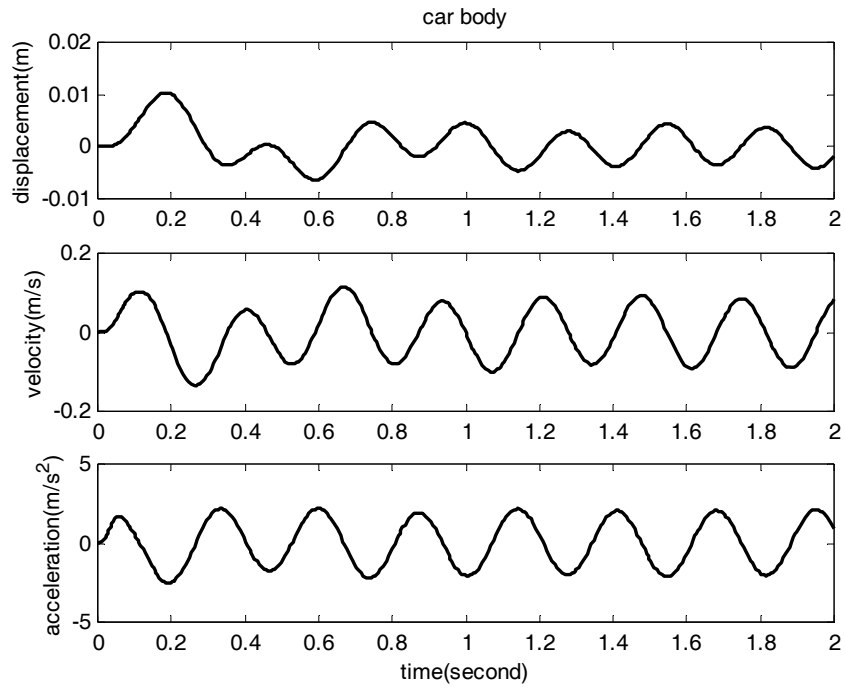Figure 4.6. Plot of the displacements vs time for unloaded FE model (V=120 km/h)

Figure 4.7. Plot of the displacement, velocity, and acceleration vs time for unloaded
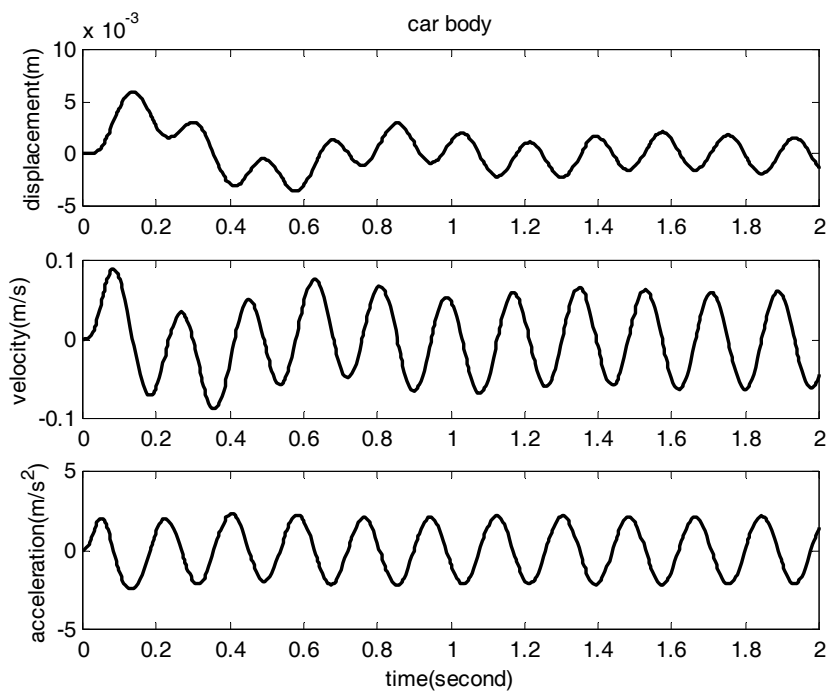FE model (V=80 km/h)

Figure 4.8. Plot of the displacement, velocity, and acceleration vs time for unloaded
FE model (V=120 km/h)

4.4. Results of the Vibration Analysis of the Finite Element Model of the Suspension System under the Axial Loads

The same physical properties of the suspension model given in Table 4.5 are considered.

4.4.1. Natural Frequencies

Under the axial loads given in Table 4.3, the natural frequencies are found as $w_1 = 8.005$ rad/s and $w_2 = 76.099$ rad/s.

4.4.2. Response to Base Excitation

Similar investigations given in Section 4.2.2 are carried out for finite element model of the suspension system with loaded links (links are loaded by joint forces). The results are presented in Figures 4.9-4.12.
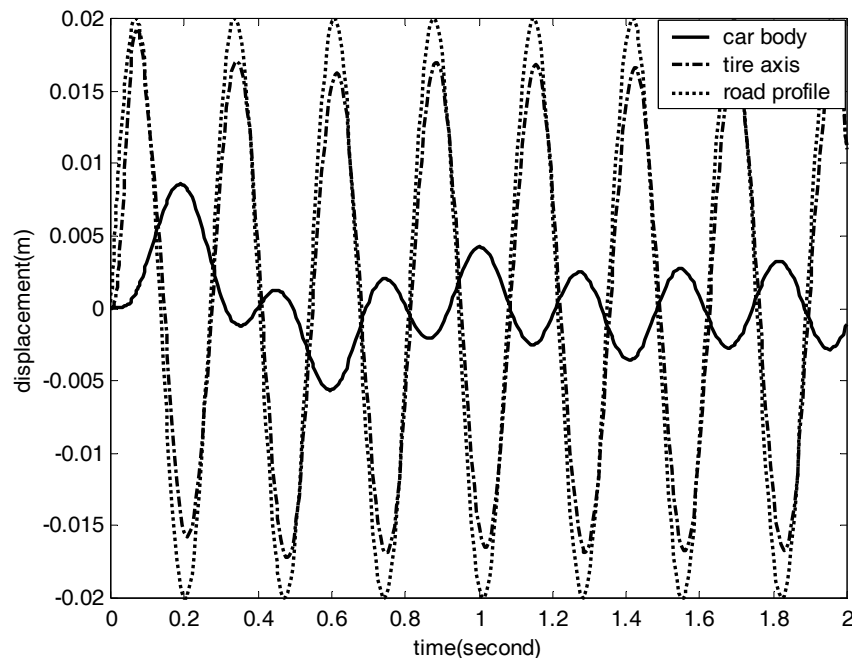
Figure 4.9. Plot of the displacements vs time for loaded FE model (V=80 km/h)
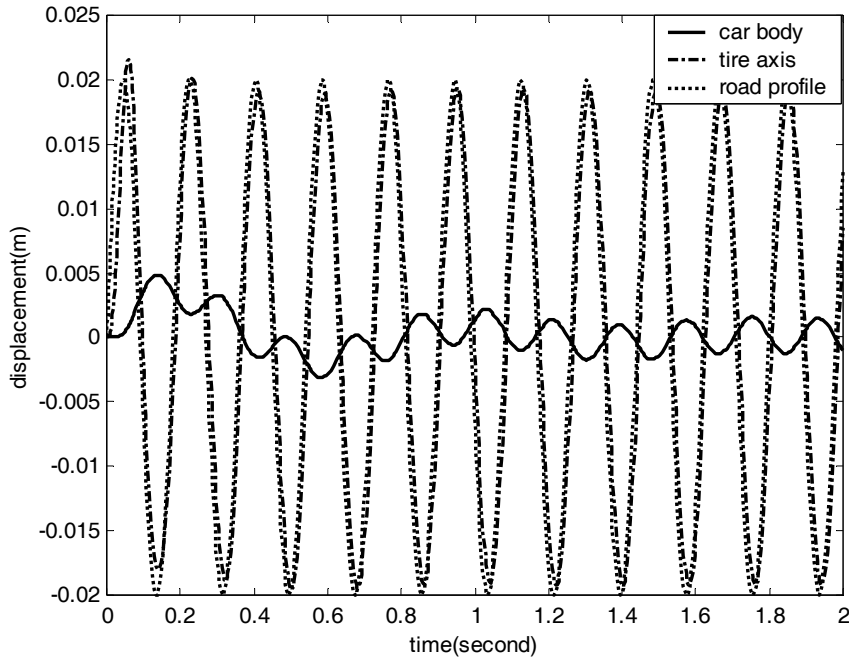
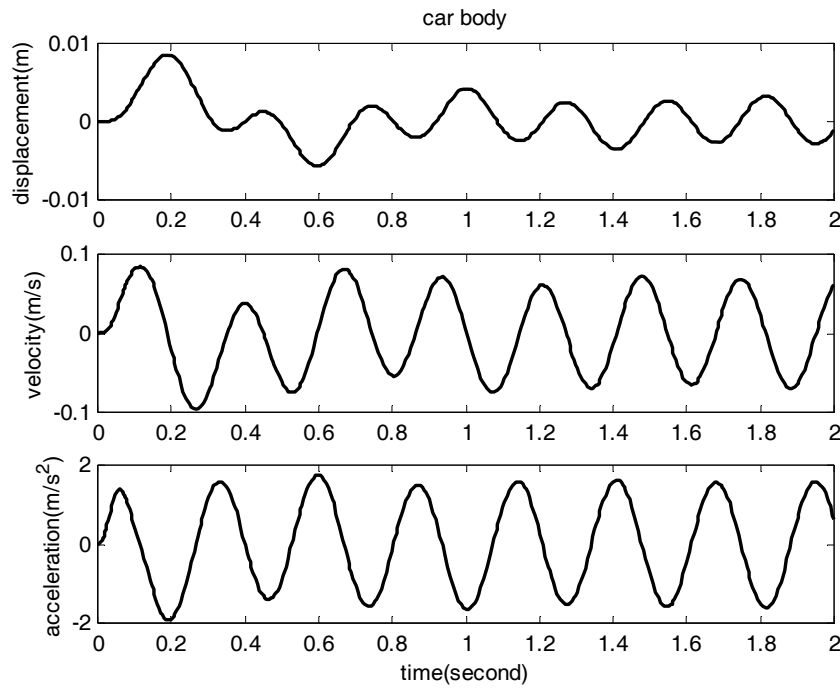Figure 4.10. Plot of the displacements vs time for loaded FE model (V=120 km/h)

Figure 4.11. Plot of the displacement, velocity, and acceleration vs time for loaded
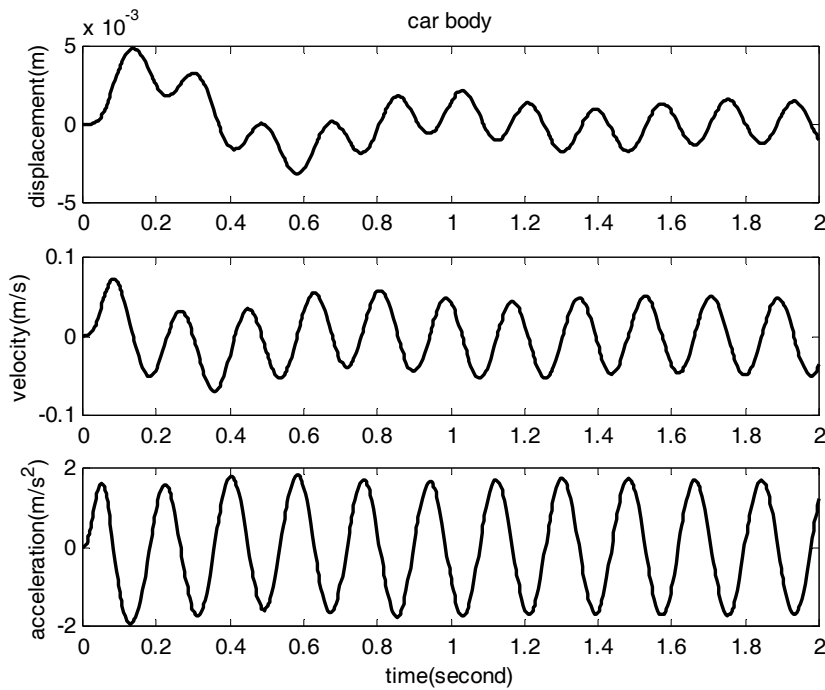
FE model (V=80 km/h)

Figure 4.12. Plot of the displacement, velocity, and acceleration vs time for loaded
FE model (V=120 km/h)

4.5. Comparisons and Discussions of Results

The effect of flexibility of the suspension links are examined for the natural frequencies. It may be noted that the natural frequencies do not depend on the link flexibilities strongly. Moreover, they are close to each others. On the other hand, the axial loads acting on the suspension links are reasonably effective on the natural frequencies of the system.

It can be seen from Figures 4.1-4.2 that when the speed of the car increases, the amplitude of the car body decreases. Also, it can be seen from the same figures that the displacements amplitude of the car body is lower than those of the tire.

It is observed from the Figures 4.1, 4.5, and 4.9 (V=80 km/h) or Figures 4.2, 4.6, and 4.10 (V=120 km/h) that the displacements amplitude of the car body for all model are close to each others for the specified car speed. Similar observation can be made for the velocity and acceleration magnitudes of the car from the Figures 4.3, 4.7, and 4.11 (V=80 km/h) or Figures 4.4, 4.8, and 4.12 (V=120 km/h).

CHAPTER 5

CONCLUSION

The effects of link flexibilities and axial link loads on the natural frequencies and also the vibration displacements, velocities, and accelerations of the car body for different double wishbone suspension models under typical sinusoidal base excitations have been analysed.

The quarter car with the double wishbone suspension system has been modelled for two different approaches to the suspension links to be rigid and flexible. Therefore, the dynamic analyses of these models have been investigated by the analytic method and the finite element method. Matlab computer programs have been developed for numerical calculations.

In the first model the link flexibilities are not included due to modelling approach. However, in the second model, finite element model, the suspension link flexibilities and the axial loads acting on suspension links are taken into account to find the natural frequencies and the time response under base excitations.

Analysis of the results showed that the agreement between the simple model and flexible model without unloaded links is excellent for both natural frequencies and the time reponses. Therefore, the simple model is adequate for the first design step. However, in order to obtain the more accurate results, for example natural frequencies and time responses, it is necessary to consider the finite element model of the suspension system.

REFERENCES

Attia, H.A., 2002. "Dynamic Modelling of the Double Wishbone Motor Vehicle Suspension System", *European Journal of Mechanics A/Solids*, Volume 21, pp.167-174.

Chandrupatla, T.R. and Belegundu, A.D., 1997. "Beams and Frames", in *Introduction to Finite Elements in Engineering*, (Prentice-Hall Inc., Upper Saddle River), p.238.

Chopra, A.K., 1995. "Damping in structures", in *Dynamics of Structures*, (Prentice-Hall Inc., Upper Saddle River, New Jersey), pp.409-429.

Cook, R.D., Malkus, D.S. and Plesha, M.E., 1989. "Stress Stiffening and Buckling", in *Concepts and Applications of Finite Element Analysis,* (John Wiley&Sons, NewYork), pp.429-448.

Esat, İ, 1999 "Genetic Algorithm Based Optimization of A Vehicle Suspension System*", Int. J. Vehicle Design*, Vol. 21, Nos.2/3, pp.148-160.

Gillespie, T.D., 1992. "Suspensions", in *Fundamentals of Vehicle Dynamics*, (Society of Automotive Engineers, USA), pp.97-117 and pp.237-247.

Gobbi M. and Mastinug G., 2001 "Analytical Description and Optimization of the Dynamic Behaviour of Passively Suspended Road Vehicles", *Journal of Sound and Vibration*, 245(3), pp.457-481.

Inman, D.J., 1996. "Response to Harmonic Excitation", in *Engineering Vibration,* (Prentice Hall, Upper Saddle River), pp.60-111.

Kwon, Y.W. and Bang, H., 1997. "Beam and Frame Structures", in *The Finite Element Method using Matlab*, (CRC Press Inc, USA), pp.259-264.

Milliken, W.F. and Milliken, D.L., 1995. "Historical Note On Vehicle Dynamics Development" and "Suspension Geometry", in *Race Car Vehicle Dynamics*, (Society of Automotive Engineers, USA), pp.413-607.

Petyt, M., 1990. "Forced Response 1 and Forced Response 2", in *Introduction to Finite Element Vibration Analysis*, (The Bath Press, Great Britain), pp.386-450.

Reimpell, J., 1973. "Krafte in der Doppel-Querlenker-Radaufhangung", in *Fahrwerktechnik 2*, (Vogel-Verlag, Germany), pp.86-99.

Remling, J., 1983. "Independent Front Suspension Systems", in *Steering and Suspension*, (Wiley, NewYork), pp.189-198.

Ünlüsoy, S., 2000. "Vehicle Suspensions and Vehicle Ride" in *Automotive Engineering 2 Lecture Notes*, Chapter V-VI.

Wang, F., 2001. "Passive Suspensions", in *Design and Synthesis of Active and Passive Vehicle Suspensions*, PhD Thesis, Control Group Department of Engineering University of Cambridge, p.85.

Wong, J.Y., 1993. "Vehicle Ride Characteristics", in *Theory of Ground Vehicles,* (John Wiley & Sons, Canada), pp.348-392.

Yamanaka, T., Hoshino, H., and Motoyama, K., 2000. "Design Optimization Technique for Suspension Mechanism of Automobile", FISITA World Automotive Congress, Seoul, (12 June -15 June 2000), Korea, pp.1-14.